Isothermal Crystallization Kinetics and Melting Behavior of Polyamide 11/Silica Nanocomposites Prepared by *In Situ* Melt Polymerization

Yunsheng Zhang,[1] Biaobing Wang,[1,2] Guosheng Hu[1]

[1]*School of Materials Science and Engineering, North University of China, Taiyuan 030051, China*
[2]*School of Materials Science and Engineering, Changzhou University, Changzhou 213164, China*

Received 18 October 2010; accepted 4 March 2011
DOI 10.1002/app.34481
Published online 26 July 2011 in Wiley Online Library (wileyonlinelibrary.com).

ABSTRACT: Polyamide 11 (PA 11)/silica nanocomposites were prepared via *in situ* melt polymerization by the dispersion of hydrophobic silica in 11-aminoundecanoic acid monomer. Their isothermal crystallization process and melting behaviors were analyzed by differential scanning calorimetry. The isothermal crystallization kinetics was analyzed by the Avrami equation. The obtained data showed that the model of nucleation and growth of PA 11 was not affected after the incorporation of silica and was a mixture with two-dimensional, circular, three-dimensional growth with thermal nucleation. Double and single melting peaks were observed depending on the crystallization temperature. The equilibrium melting point of samples was evaluated, and the spherulites growth kinetics parameters and fold surface free energy were further calculated according to the classical theories. © 2011 Wiley Periodicals, Inc. J Appl Polym Sci 123: 273–279, 2012

Key words: polyamide 11; silica; nanocomposites; isothermal crystallization; melting behavior

INTRODUCTION

Recently, polyamide 11 (PA 11) has attracted much attention as one of the promising engineering plastics, which can be produced from renewable resources. Because of its excellent piezoelectric behavior and good cryogenic and low moisture sorption properties, PA 11 is widely used in industrial fields from automotive to offshore oilfield applications. Many efforts have been made to improve its mechanical properties, ferroelectric, and piezoelectric property or to reduce its yield cost.[1–6] Preparing blends using nanofillers offers a promising method to improve properties of polyamides. Some works have been reported on the preparation and properties of PA 11–based nanocomposites.[7–9] To the best of our knowledge, there is no literature on the modification of PA 11 with silica nanoparticle. In our laboratory, PA 11/silica nanocomposite was prepared by *in situ* melt polymerization.

It is well understood that physical, chemical, and mechanical properties of crystalline polymer depend strongly on the morphology, crystalline structure, and degree of crystallization, which in turn is significantly controlled by the crystallization process during the solidification process. Hence, the study of the kinetics of crystallization is necessary for optimizing the process conditions and establishing the structure–property correlations in polymers. The crystallization behavior and crystal structure of nylon 11 have been investigated by many researchers.[10–12] The crystallization behavior of PA 11–based nanocomposites has also been studied to explore the effect of nanofillers on the macroscopic performance of naonocomposites.[13,14] It has been demonstrated that the nanofillers can promote the crystallization of polymer matrix in low content, whereas it impedes the crystallization at higher loading. In this article, the isothermal crystallization behaviors of PA 11/silica nanocomposites were investigated using differential scanning calorimetry (DSC). The melting behaviors after the completion of isothermal crystallization process were also discussed. The equilibrium melting temperature, spherulites growth kinetics parameter, and fold surface free energy were determined according to classical theories.

MATERIALS AND EXPERIMENTAL

Materials

11-Aminoundecanoic acid was kindly provided by ZhongLian Zenong Chemical Engineer (Taiyuan, China) and was used without purification.

Correspondence to: B. Wang (bbwang@nuc.edu.cn).
Contract grant sponsor: Key Science and Technology Project of Shanxi Province; contract grant number: 20100321081.
Contract grant sponsor: Department of Personnel of Shanxi Province (Special Funding for Talent Introduction and Development).

Hydrophobic nanosilica was prepared via the vitriol precipitation method using cheaper water glass as raw material in our laboratory, and the average size of nanosilica agglomerates was 264.8 nm with narrow distribution. 11-Aminoundecanoic acid and hydrophobic nanosilica (coated with silane coupling agent) were dried at 80°C in vacuum for at least 12 h before synthesis.

In situ synthesis of PA 11/silica nanocomposites

The weighted 11-aminoundecanoic acid and hydrophobic nanosilica were blended using a high-speed mixer, and the mixture was added into a 150-mL ampoule tube connected with a vacuum/inert gas joint. Oxygen and volatile was removed repeatedly by degassing the mixture using an inert gas (nitrogen) for several times. The ampoule tube was heated to 190°C and reacted for 2 h. The reactor is then heated to 230°C, and the polymerization was kept under vacuum for 2–6 h at 230°C. After the completion of polymerization, the ampoule tube was cooled to room temperature, and the production was granulated. The *in situ* synthesized PA 11/silica nanocomposites were abbreviated as NC-X, wherein X denotes the weight percentage of nanosilica.

The molecular weight of samples was controlled to be as uniformly as possible to eliminate the possible effect on crystallization by adjusting the synthesis time. The intrinsic viscosity of the pure PA 11, NC-5, and NC-8 was 0.95, 0.93, and 0.92 dL/g, respectively.

DSC analysis

Isothermal crystallization and subsequent melting behavior studies were performed using a Mettler DSC822e, and the temperature was calibrated with the indium standard. All DSC experiments were performed under a nitrogen purge at a constant flow rate. Sample weights were between 2 and 3 mg. All samples were dried at 80°C under vacuum for 12 h before measurement.

DSC experiments of isothermal crystallization and subsequent melting behaviors were performed as follows: the sample was heated to 230°C at a rate of 50°C/min and stayed for 10 min to eliminate any previous thermal history. Then, it was cooled at a rate of −100°C/min to the predetermined crystallization temperature (T_c) and was maintained at T_c for 1 h. The specimens were subsequently heated to 230°C at a rate of 10°C/min.

RESULTS AND DISCUSSION

Melting behaviors after isothermal crystallization

The DSC heating thermograms of PA 11 and its nanocomposites after crystallization at various T_c was illustrated in Figure 1. Double melting peaks were observed for all samples in the case of low crystallization temperatures. The Peak I at lower temperature shifts toward a higher temperature as the crystallization temperature increases, whereas the Peak II at high temperature becomes weaker, but its position displays almost no change. Such double melting endotherms can be contributed to two different crystal structures, different crystal size and perfection, or recrystallization.[15,16] The melting Peak I is assumed to be caused by the melting of crystals formed on cooling from melt, whereas the Peak II mainly corresponds to the melting of crystals that have recrystallized during the heating run (after the first melting peak). More perfect crystals are formed at high crystallization temperature, and they start to melt at higher T_c. When the perfection of crystals is no more improved with increasing T_c, no further recrystallization takes place during the DSC run, resulting in the two peaks merging into a single one for the samples crystallized at higher temperature.

Equilibrium melting temperature

To carry on quantitative analysis of crystallization behavior, especially to investigate the temperature dependence of the crystallization rate, it is necessary to determine the equilibrium melting point as accurately as possible. According to the Hoffman–Weeks theory,[17] the equilibrium melting point (T_m^0) can be determined by linear extrapolation of T_m versus T_c data to intersect the line $T_m = T_c$. Mathematically, the dependence of T_m on T_c is expressed as:

$$T_m = \frac{T_c}{2\beta} T_m^0 \left(1 - \frac{1}{2\beta}\right) \quad (1)$$

where $\beta = \sigma_e l / \sigma l_e$, and σ is the fold surface free energy, l is the lamellae thickness and the subscript e refers to equilibrium conditions, and $\beta = 1.0$ in the absence of recrystallization or annealing during melting.[18,19]

It is well known that the higher the crystallization temperature, the more suitable it is to get the equilibrium melting point.[20] Because the high temperature peaks are approximately at the same position regardless of the temperatures at which the samples were crystallized. Therefore, the value of melting temperature at Peak I according to low T_c and those melting temperature obtained when only single melting peak was plotted as a function of T_c in Figure 2. Extrapolating linearly the experimental data up to the $T_m = T_c$ line according to Hoffman–Weeks analysis, the equilibrium melting temperature (T_m^0) for the pure PA 11, NC-5, and NC-8 are determined to be 225.09, 206.03, and 205.60°C, respectively. The T_m^0 value of the pure PA 11 was higher

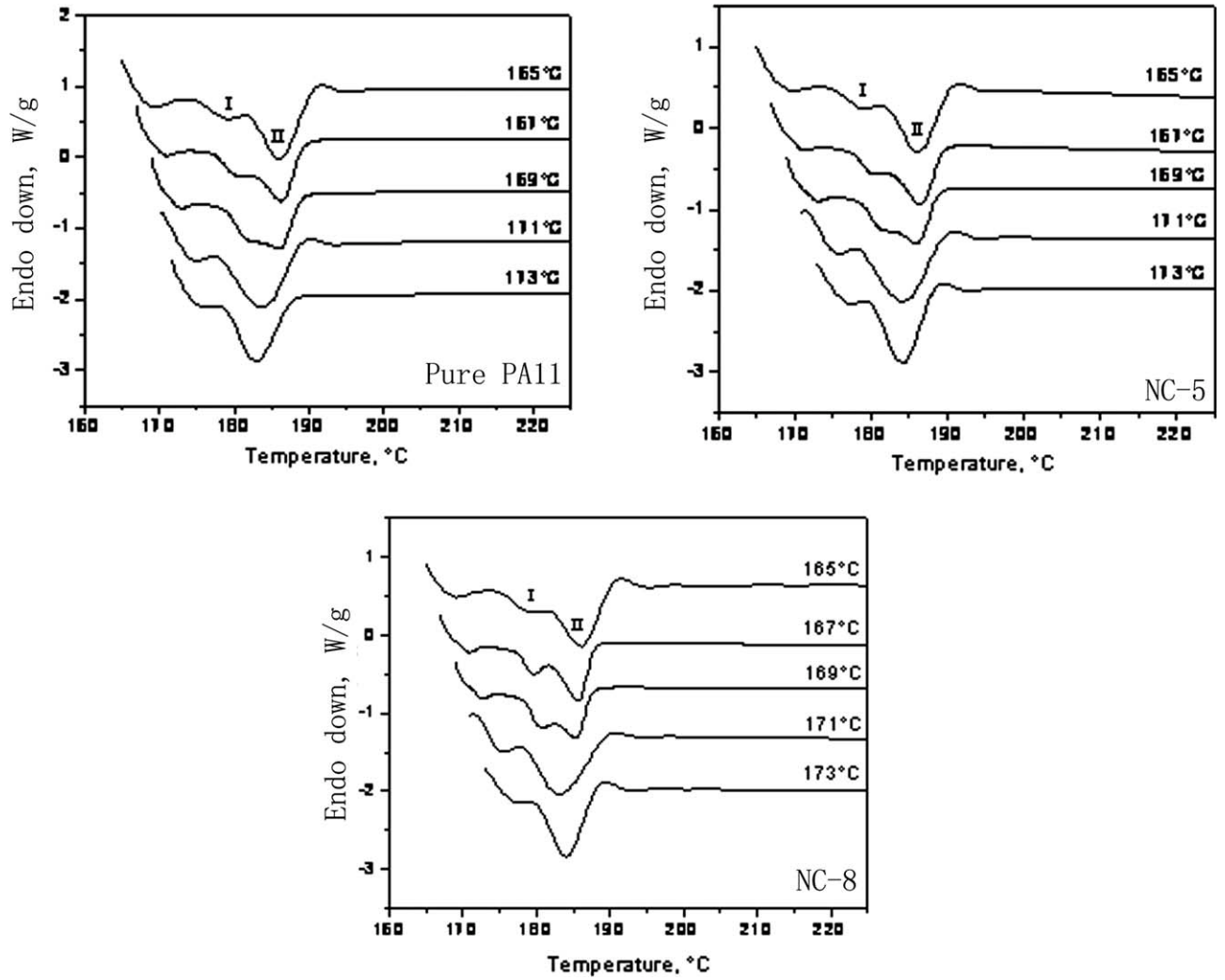

Figure 1 DSC traces of samples isothermally crystallized at the indicated temperatures at heating rate of 10°C/min.

than that reported by Liu et al.[11] and Zhang et al.[21] In addition, the nanocomposites display lower T_m^0 values compared with the pure PA 11, indicating that the crystals in the nanocomposites become imperfect because of the retarded crystallization phenomena induced by the incorporation of silica.

Isothermal crystallization behavior

The crystallization behavior of all specimens was carefully investigated by DSC. Figure 3 shows a typical DSC trace of NC-5 that isothermally crystallized at the predetermined temperatures. As can be seen, the crystallization peaks shift toward to the right and become flatter with the increasing crystallization temperature. It implies that the crystallization rate decreases with the increasing crystallization temperature.

Isothermal crystallization kinetics analysis

With the recorded DSC exothermic curves in terms of the heat flow per gram of the sample $dH(t)/dt$ as a function of time for systems undergoing the isothermal crystallization process at various T_c, we can analyze the isothermal crystallization kinetics. The relative degree of crystallinity at different crystallization time can be calculated according to the following equation[22]:

$$X(t) = \frac{X_c(t)}{X_c(t=\infty)} = \frac{\int_0^t \frac{dH_c(t)}{dt}dt}{\int_0^{t=\infty} \frac{dH_c(t)}{dt}dt} \quad (2)$$

where $X_c(t)$ and $X_c(t=\infty)$ is the relative degree of crystallinity at time t and infinite time, respectively. The plot of $X(t) \sim t$ for NC-5 is shown typically in Figure 4. It is clear that characteristic sigmoid isotherms shift to the right with the increasing isothermal crystallization temperature. The completion time of crystallization becomes longer, and the crystallization rate decreases.

Assuming the relative degree of crystallinity increases with an increase in the crystallization time, the Avrami equation is adopted to analyze the isothermal crystallization process[23,24]:

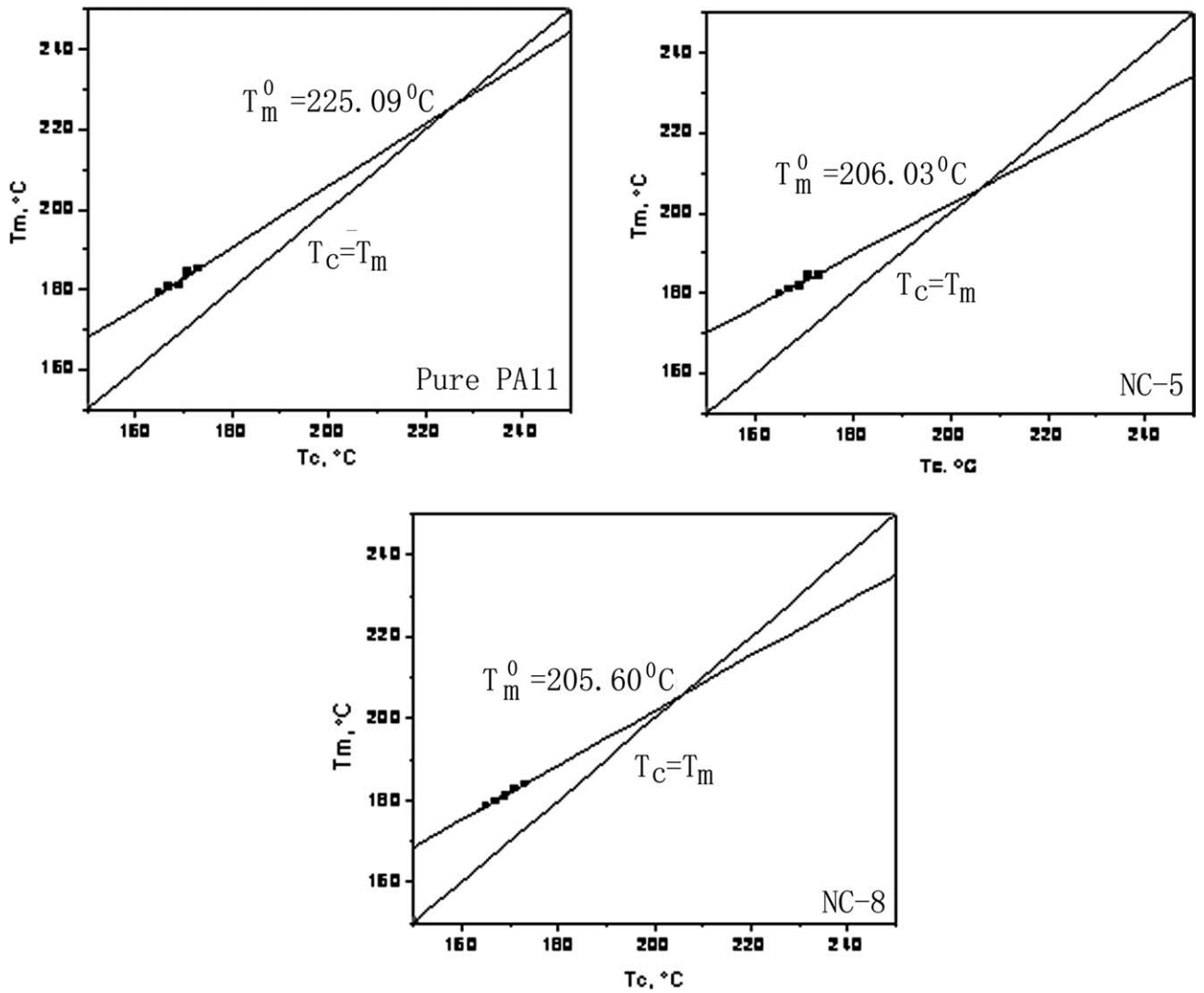

Figure 2 Application of Hoffman–Weeks analysis to samples for determining equilibrium melting temperature. Melting point of Peak I as a function of the crystallization temperature.

$$X(t) = 1 - \exp(-\mathrm{K}t^n) \tag{3}$$

or

$$\log[-\ln(1 - X(t))] = n \log t + \log K \tag{4}$$

where K is the crystallization rate constant, and n is the Avrami exponent whose value depends on the mechanism of nucleation and on the form of crystal growth. The plot of $\log\{-\ln[1 - X_c(t)]\}$ versus log$t$ for NC-5 is illustrated typically in Figure 5. Unlike most semicrystalline polymers, no obvious roll-off at longer times is observed, implying that the secondary crystallization of PA 11in the nanocomposites does not occur under experimental conditions. For comparison, the regime of about 10–75% conversion in the curves for the samples is chosen to determine the exponent n and K according to eq. (4). Performing the least square fit to the linear section in Figure 5, the values of n and K (Table I) are obtained from the slope

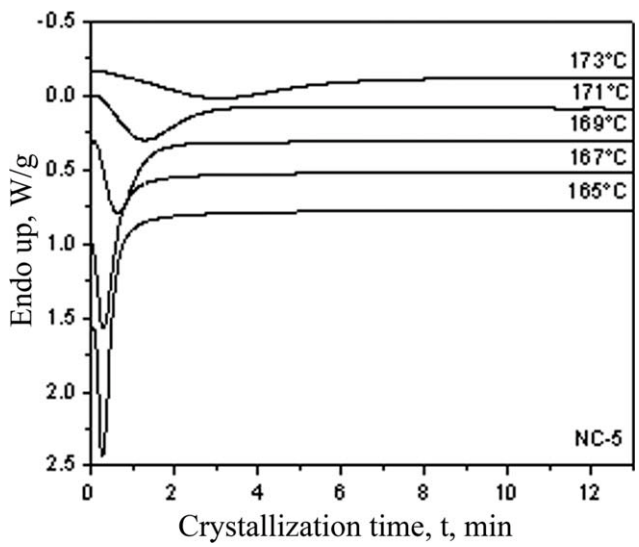

Figure 3 DSC traces of samples isothermally crystallized at the indicated temperatures.

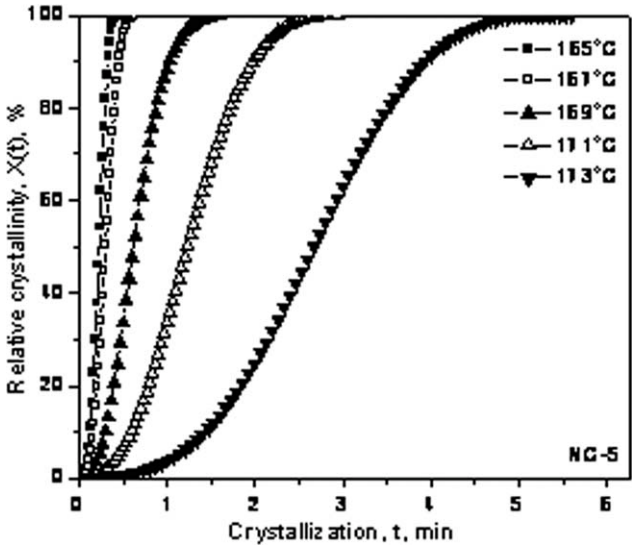

Figure 4 Relative crystallinity $X(t)$ versus different crystallization time t in the isothermal crystallization process for NC-5 sample.

and intercept of the fitted curves, respectively. Usually, the values of n should be an integer between 1 and 4 for different crystallization mechanisms. Because other complex factors, such as the competition of a diffusion-controlled growth and the irregular boundary of the spherulites, are probably involved during the process, the Avrami exponent n is not a straightforward integer.[25] It can be seen that the obtained values of n for all samples are similar at the same crystallization temperature, indicating that the model of nucleation and growth of PA 11 is not affected after the incorporation of silica. In addition, all the n values fall into the range of 2.37 and 3 0.39, showing that the crystallization model of PA 11 might be a mixture with two-dimensional, circular, three-dimensional growth with thermal nucleation.[26] The values of the crystallization rate parameter K for all samples increase with decreasing crystallization temperature. Moreover, the K value of nanocomposites is greater than that of the pure PA 11 at the same indicated T_c and tends to increase with the further loading of silica. It is implied that silica can act as heterogeneous nucleating agent and promote the crystallization process.

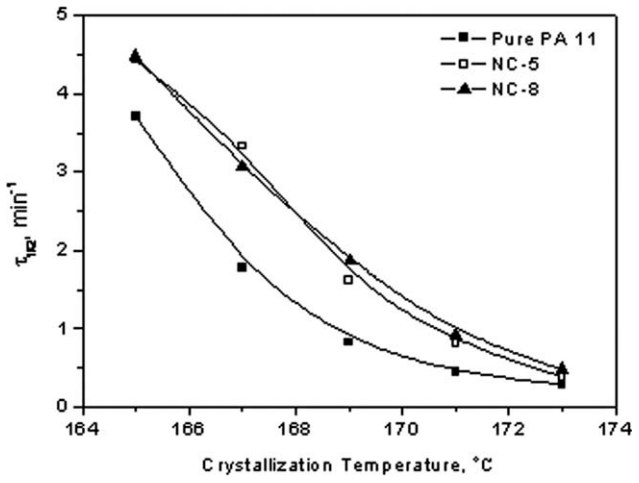

Figure 5 Crystallization rate as a function of crystallization temperature for samples.

Some other important parameters for the crystallization kinetics include crystallization half-time, rate of crystallization, and the time for maximum crystallization.

The crystallization half-time $t_{1/2}$ is defined as the time at which the relative degree of crystallinity was 50% and can be calculated from eq. (5) using the measured kinetics parameters,

$$t_{1/2} = (\ln 2/K)^{1/n} \tag{5}$$

The rate of crystallization G is defined as the reciprocal of $t_{1/2}$; that is, $G = \tau_{1/2} = 1/t_{1/2}$.[27] We find in the curves of G versus T_c (Fig. 6) that the rate of crystallization decreases with increasing T_c for each specimen. Furthermore, the rate of crystallization displays an increasing behavior with the increasing silica loading level. It was speculated that the separated silica nanoparticles can act as heterogeneous nucleating site, which results in a faster nucleation rate.

The time to reach the maximum rate of crystallization t_{max} can also be used to characterize the rate of crystallization. The data of t_{max} can be readily obtained from the isotherms in Figure 3.[28] Because t_{max} corresponds to the point at which $dQ(t)/dt = 0$, $Q(t)$ is the rate of heat evolution, thus t_{max} can be determined as follows:

$$t_{max} = [(n-1)/nK]^{1/n} \tag{6}$$

TABLE I
Parameters of the Isothermal Crystallization for Pure PA 11 and its Nanocomposites

Sample	T_c (°C)	n	K (min^{-1})	$t_{1/2}$ (min)	$\tau_{1/2}$ (min^{-1})	t_{max} (min)
PA 11	165	2.84	28.49	0.27	3.71	0.26
	167	2.73	3.29	0.57	1.77	0.55
	169	2.91	0.39	1.22	0.82	1.20
	171	3.37	0.04	2.27	0.44	2.28
	173	2.88	0.02	3.56	0.28	3.49
NC-5	165	3.29	92.28	0.23	4.43	0.23
	167	2.85	21.30	0.30	3.33	0.29
	169	2.49	2.26	0.62	1.61	0.59
	171	2.55	0.41	1.23	0.81	1.17
	173	3.06	0.03	2.67	0.38	2.64
NC-8	165	3.39	110.98	0.22	4.48	0.22
	167	2.55	11.99	0.33	3.06	0.31
	169	2.37	3.04	0.54	1.87	0.49
	171	2.37	0.58	1.08	0.92	1.00
	173	2.69	0.09	2.09	0.48	2.02

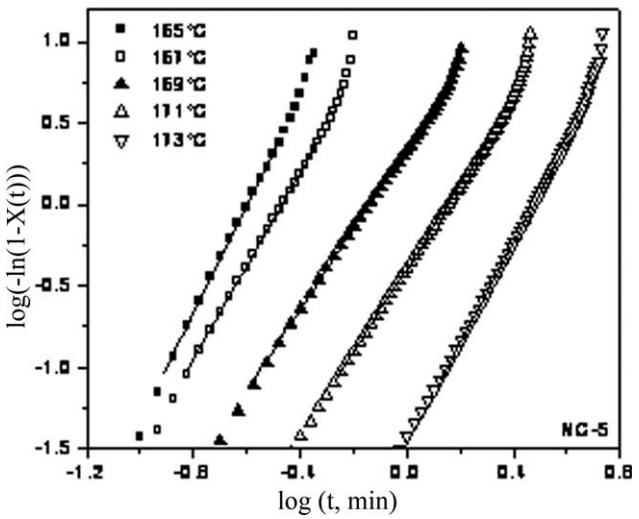

Figure 6 A typical plot of $1g(-\ln(1 - X(t)))$ versus $1g(t)$ of the NC-5 sample isothermally crystallized at the predetermined temperatures.

The value of t_{max} can be derived from the Avrami exponent n and the parameter K, as summarized in Table I.

Nucleation parameter and surface free energy

The Hoffman–Lauritzen theory[29] suggests that the linear growth rate, G, depends on temperature, T, as follows:

$$G = G_0 \exp\left(\frac{-U^*}{R(T_c - T_\infty)}\right) \exp\left(\frac{-K_g}{T_c \Delta T f}\right) \quad (7)$$

or

$$\ln G + \frac{U^*}{R(T_c - T_\infty)} = \ln G_0 - \frac{K_g}{T_c \Delta T f} \quad (8)$$

The first exponential terms describes the effect of the temperature dependence of melt viscosity and accounts for the reduced molecular mobility as the temperature approaches the glass transition temperature, and in particular, the thermodynamic glass transition temperature $T_\infty = T_g - 30$ ($T_g = 43°C$ for PA 11 in this study). This term also contains the activation energy for chain transport and viscous flow U^*, for which is commonly given by a universal value of 6300 J/mol. The second exponential terms accounts for the rate determining effect of primary nucleation on the crystallization at low degree of supercooling ($\Delta T = T_m^0 - T_c$). The parameter $f = 2T_c/(T_m^0 + T_c)$ is a correction factor that accounts for the change in the latent heat of fusion that occurs with changing crystallization temperatures.

The kinetic parameter, K_g, is a term connected with the energy need for the formation of nuclei of critical size and has the following form:

$$K_g = \frac{nb\sigma\sigma_e T_m^0}{\Delta h_f k_B} \quad (9)$$

where b is the distance between two adjacent fold planes, σ and σ_e are the lateral and fold surface free energy, k_B is the Boltzmann constant, Δh_f is the heat of fusion per unit volume of crystal, and n takes the value 4 for crystallization Regimes I and III and 2 for regime II. In the current work, the crystallization Regime I was observed, and n took the value 4. The results of the kinetic data treatment, using G values presented in Figure 6, are illustrated in Figure 7. The values of the nucleation parameter K_g are given as a slope of 5.76×10^5 K^2, 2.31×10^5 K^2, and 2.03×10^5 K^2 for pure PA 11, NC-5, and NC-8, respectively. Clearly, the K_g values of the nanocomposites are lower than those of the pure PA 11 and tend to decrease with the further loading of silica. Generally, a foreign surface reduces frequently the nucleus size for crystal growth because the creation of the interface between polymer crystal and substrate may be less hindered than the creation of the corresponding free polymer crystal surface. A preexisting surface can reduce the free energy opposing primary nucleation for a heterogeneous nucleation process. As such, the well-separated silica nanoparticles can reduce the work necessary to create a new surface.

Adoption $\Delta h_f = 2.1797 \times 10^8$ J/m^3 and $b = 4.44$ Å,[30] the production of $\sigma\sigma_e$ can be evaluated from eq. (9). The data of $\sigma\sigma_e$ for the pure PA 11, NC-5, and NC-8 are 1.96×10^{-3} J^2/m^4, 0.82×10^{-3} J^2/m^4, and 0.72×10^{-3} J^2/m^4, respectively.

σ was often estimated by an empirical equation as follows[31]:

$$\sigma = 0.11 \Delta h_f \sqrt{a_0 b_0} \quad (10)$$

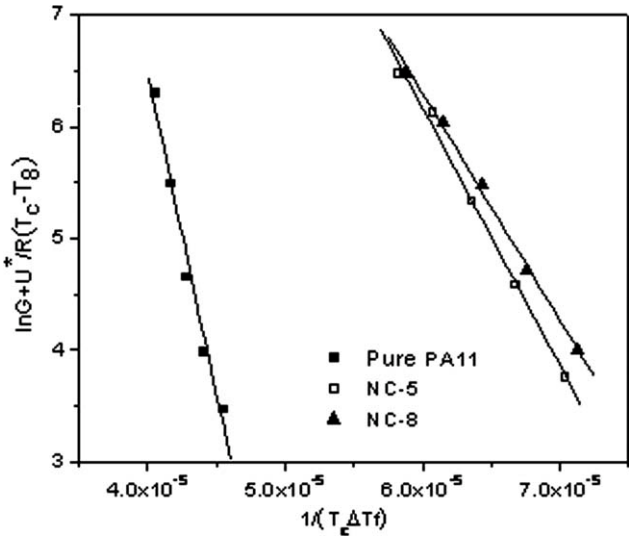

Figure 7 Plots of $\ln G + U^*/R$ ($T_c - T_\infty$ versus $1/(T_c \Delta T f)$ for samples.

where a_0 and b_0 are the parameters of the PA 11 unit cell, and their values are 4.9 and 5.4 Å, respectively. σ is thus determined to be 1.23×10^{-2} J/m^2. Substituting this value into $\sigma\sigma_e$, the fold surface free energy (σ_e) for the pure PA 11, NC-5, and NC-8 are obtained to be 0.159, 0.067, and 0.059 J/m^2, respectively. The lower the values of σ_e, the less the necessary energy for the fold of the macromolecules into the nucleus surface. Therefore, the values of σ_e for the pure PA 11 and its nanocomposites indicate that the macromolecules can readily fold into the nucleus surface with the incorporation of silica, which promote the crystallization process. The results are in good agreement with that obtained from Avrami equation.

CONCLUSIONS

The isothermal crystallization and melting behaviors of the *in situ* synthesized PA 11/silica nanocomposites were analyzed by DSC. The Avrami equation well described the isothermal crystallization process of the primary stage. The data obtained from the analysis of isothermal process showed that the incorporation of nanosilica has no significant influence on the crystallization model of PA 11 but promoted the rate of crystallization. The evaluation of the spherulites growth kinetics parameters and fold surface free energy further supported this result.

All specimens displayed double melting peaks after isothermally crystallized at the lower temperature, whereas single melting peaks after isothermally crystallized at the higher temperature. The equilibrium melting point was further evaluated according to the classical theory.

References

1. Zhou, C. J; Wang, K.; Fu, Q. Polym Int 2009, 58, 538.
2. Hu, G.; Wang, B.; Zhou, X. Polym Int 2005, 54, 316.
3. Li, Q.; Tian, M.; Kim, D.; Wu, D.; Jin, R. J Appl Polym Sci 2002, 83, 1600.
4. Fabien Capsal, J.; Pousserot, C.; Dantras, E.; Dandurand, J.; Lacabanne, C. Polymer 2010, 51, 5207.
5. Tsutsumi, N.; Yamaoka, T. Thin Solid Films 2009, 518, 814.
6. Wang, B.; Hu, G.; Zhao, X.; Gao, F. Matter Lett 2006, 60, 2715.
7. Liu, T.; Lim, K.; Tjiu, W.; Pramoda, K.; Chen, Z. Polymer 2003, 44, 3529.
8. Zhang, X.; Yang, G.; Lin, J. J Polym Sci B: Polym Phys 2006, 44, 2161.
9. Huang, S.; Wang, M.; Liu, T.; Zhang, W.; Ljiu, W.; He, C.; Lu, X. Polym Eng Sci 2009, 49, 1063.
10. Nair, S. S.; Ramesh, C.; Tashiro, K. Macromol Symp 2006, 242, 216.
11. Liu, S.; Yu, Y.; Cui, Y.; Zhang, H.; Mo, Z. J Appl Polym Sci 1998, 70, 2371.
12. Zhang, Q.; Mo, Z.; Zhang, H.; Liu, S.; Cheng, S.Z.D. Polymer 2001, 42, 5543.
13. Ma, Y.; Hu, G.; Ren, X.; Wang, B. Mater Sci Eng A 2007, 460–461, 611.
14. Zhang, X.; Yang, G.; Lin, J. J Appl Polym Sci 2006, 102, 5483.
15. Takase, Y.; Lee, J. W; Scheinbeim, J. I.; Newman, B. A. Macromolecules 1991, 24, 6644.
16. Scheinbeim, J. I.; Lee, J. W.; Newman, B. A. Macromolecules 1992, 25, 3729.
17. Hoffman, J. D.; Weeks, J. J. J Res Natl Bur Stand 1962, 66A, 13.
18. Jenkins, M. J Polym 2001, 42, 1981.
19. Wunderlish, B. Macromolecular Physics; Academic Press: New York, 1980.
20. Wang, G. M.; Yan, D. Y.; Bu, H. S. Chin J Polym Sci 1998, 16, 2642.
21. Zhang, X. K.; Xie, T. X.; Yang, G. S. Polymer 2006, 47, 2116.
22. Cebe, P.; Hong, S. D. Polymer 1986, 27, 1183.
23. Avrami, M. J Chem Phys 1939, 7, 1103.
24. Avrami, M. J Chem Phys 1940, 8, 212.
25. Shultz, J. Polymeric Material Science; Prentice-Hall: New York, 1974.
26. Zhang, Q. X.; Zhang, Z. H.; Zhang, H. F.; Mo, Z. S. J Polym Sci Part B: Polym Phys 2002, 40, 1784.
27. Hoffman, J. D.; Davis, G. T.; Lauritzen, J. I. In Treatise on Solid State Chemistry: Crystalline and Non-crystalline Solids; Hannary, N. B., Ed.; Plenum: New York, 1976.
28. Lin, C. C. Polym Eng Sci 1983, 23, 113.
29. Hoffman, D. J.; Davis, G. T., Lauritzen, J. I. Treatise on Solid State Chemistry; Hammay, N. B., Ed.; Plenum: New York, 1976, Vol. 3, Chapter 7, p 497.
30. Liu, S.; Yu, Y.; Cui, Y.; Zhang, H.; Mo, Z. J Appl Polym Sci 1998, 70, 2371.
31. Lauritzen J. I., Jr.; Hoffman, J. D. J Appl Phys 1973, 44, 4340.